Covalent Capture and Stabilization of Cylindrical β-Sheet Peptide Assemblies

Thomas D. Clark, Kenji Kobayashi, and M. Reza Ghadiri*[a]

Abstract: The utility of noncovalent approaches to molecular self-assembly is often limited by kinetic instability of the resulting constructs. In an effort to surmount this difficulty, we have employed noncovalent interactions between self-assembling cyclic peptide subunits to direct covalent bond formation, resulting in cylindrical β-sheet dimers that are both kinetically and thermodynamically stable. In the two peptide systems examined, we found that intersubunit hydrogen bonding serves important but distinct functions. For olefin metathesis of homoallylglycine (Hag)-bearing peptide **1**, hydrogen bonding drives the reaction by increasing olefin effective molarity. In contrast, for disulfide isomerization of monomeric cystine peptide **5-SS**, hydrogen bonding appears to control partitioning between two alternative disulfide-bonded dimers by contributing to the stability of the hydrogen-bonded isomer. Our proposed mechanism for the latter transformation is reminiscent both of thiol-catalyzed unscrambling of RNase A and oxidative refolding pathways of natural proteins and protein fragments.

Keywords: β-sheets · olefin metathesis · supramolecular chemistry · template synthesis thiol–disulfide interchange

Introduction

Supramolecular approaches to self-assembly often rely upon reversible noncovalent interactions.[1, 2] Virtues of such strategies include error correction through thermodynamic equilibration, minimization of synthetic effort by use of modular subunits, control of assembly processes through subunit design, and overall high efficiency.[2] However, the equilibrium ensembles thus obtained often exhibit low kinetic stability, undergoing rapid assembly–disassembly despite thermodynamically stable assembled states. Although solid-state supramolecular chemistry (crystal engineering)[3] offers one means of overcoming this limitation, preparation of soluble or solvent-stable aggregates is often desirable. An alternative approach employs noncovalent interactions between subunits to template covalent bond formation, resulting in constructs which are both thermodynamically and kinetically stable. We term this strategy *covalent capture* and note that it represents a specialized case of template-directed synthesis in which the template is an integral part of the structure it helps to form.[4–6]

[a] Prof. M. R. Ghadiri, Dr. T. D. Clark, Dr. K. Kobayashi[+]
Departments of Chemistry and Molecular Biology and The Skaags Institute for Chemical Biology
The Scripps Research Institute
10550 N. Torrey Pines Rd.
La Jolla, CA 92037 (USA)
Fax: (+1) 619-784-2798
E-mail: ghadiri@scripps.edu

[+] Present address: Department of Chemistry, University of Tsukuba, Tsukaba, 305–8571 (Japan)

Biological systems frequently employ covalent capture to stabilize both inter- and intramolecular assemblies. Examples include buttressing of DNA structures by enzymatic ligation[7, 8] and reinforcement of protein folds by disulfide bond formation.[9–12] Inspired by the efficiency of such transformations, chemists have applied covalent capture to preparation of artificial assemblages such as molecular catenanes, rotaxanes, and knots.[13–15] Herein we describe our own investigations employing self-assembling cyclic peptide templates as simplified models of protein secondary structure.

Design Principles

Self-assembling cyclic D,L-peptide nanotubes: Recent reports have shown that cyclic peptides composed of an even number of alternating D- and L-amino acids (cyclic D,L-peptides) can adopt flat, ring-shaped conformations and stack through backbone–backbone hydrogen bonding to form large tubular aggregates.[16–22] As an extension of this work, soluble nanocylinrical constructs were prepared by selective incorporation of N-alkylated residues, thereby limiting self-assembly to formation of discrete dimeric ensembles.[23–28] Crystallographic and spectroscopic data have conclusively demonstrated that dimerization takes place through the expected antiparallel β-sheet hydrogen-bonding network, rendering dimer-forming cyclic D,L-peptides one of the most synthetically accessible and structurally well characterized β-sheet peptide scaffolds.[23–28] We therefore chose to exploit this system for our initial explorations in order to permit detailed chromato-

0947-6539/99/0502-0782 $ 17.50+.50/0

graphic and spectroscopic characterization of the covalent-capture processes. In addition, these investigations will serve as model studies for preparation of novel materials based on covalently polymerized cyclic peptide nanotubes.

Choice of covalent bond-forming processes. Figure 1 outlines our general strategy. Cyclic peptide subunits self-assemble in a nonpolar organic solvent, bringing reactive side-chain functionalities into proximity across the β-sheet hydrogen-bonding interface. Covalent bond formation then occurs, trapping and stabilizing the cylindrical peptide complex. Due to unfavorable changes in entropy associated with a decrease in the number of particles in solution, we reasoned that the cross-linked dimer would be the most thermodynamically stable product. The covalent chemistry employed must tolerate both peptide backbone functionalities as well as intersubunit hydrogen bonding. In addition, use of reversible covalent chemistry should in principle lead to error correction by allowing equilibration of unwanted intermediates to the desired thermodynamic product.[2, 6]

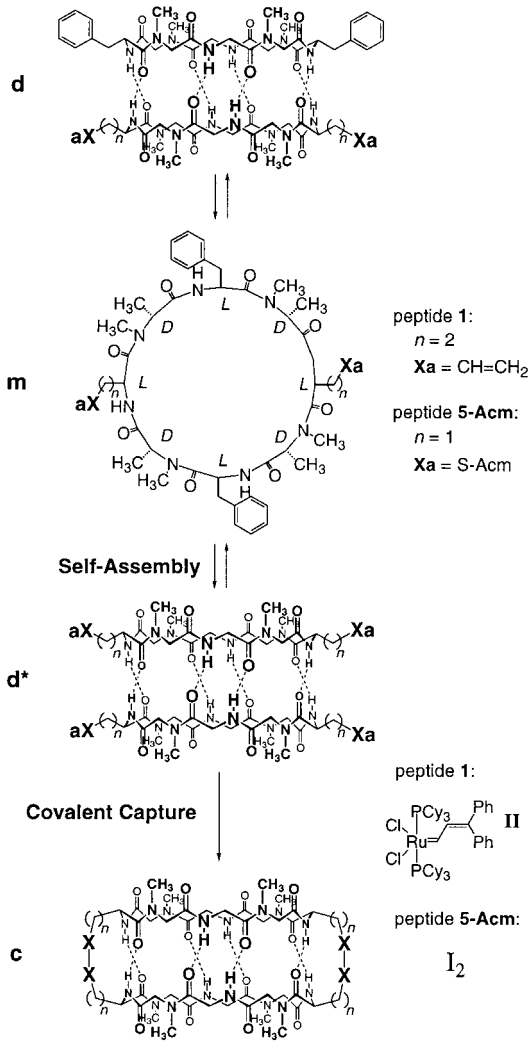

Figure 1. General strategy for covalent capture and stabilization of cylindrical β-sheet peptide assemblies. Monomeric peptide **m** dimerizes in nonpolar media to give two interconverting species **d** and **d***. In productive complex **d***, reactive side chain groups **Xa** are preorganized for intersubunit (**X–X**) bond formation, producing covalently tethered dimer **c**. For homoallylglycine (Hag) peptide **1** and acetamidomethyl cysteine ((Cys(Acm)) peptide **5-Acm**, we have investigated olefin metathesis using the selective Ru^{II} complex **II** and iodine oxidation, respectively. (For clarity, most side chains are omitted.)

On the basis of these criteria, we chose to investigate olefin metathesis catalyzed by the remarkably selective Ru^{II} complex **II** developed by Grubbs et. al. (Figure 1).[29–31] Olefin metathesis is a reversible transformation leading to thermodynamically stable products.[32] At the time of our preliminary report,[24] **II** had been shown to efficiently catalyze ring opening metathesis polymerization (ROMP) of strained cyclic olefins[31], proximity-driven ring-closing metathesis (RCM) of acyclic dienes,[31, 33–36] as well as cross metathesis of acyclic olefins, while tolerating a wide range of functionality including ether, hydroxyl, carboxylic acid, aldehyde, and amide groups. Of particular relevance to our own work, a 1995 report by Miller and Grubbs described application of RCM to synthesis of conformationally restricted amino acids and peptides.[33] Furthermore, these authors implicated intramolecular hydrogen bonding as a directing element in preparation of β-turn analogues using RCM. Thus we viewed olefin metathesis catalyzed by **II** as an intriguing transformation ideally suited to our objectives.

The design of olefin-bearing peptide **1** incorporates homoallylglycine (Hag) residues, which modeling studies suggested would offer an optimum balance between preorganization for covalent capture and low steric strain in the anticipated products (**3**, Figure 5). We predicted that the increased effective molarity of olefin groups in dimer **1-d*** would favor acyclic cross metathesis, a transformation usually requiring concentrated reaction conditions.[31, 32] Intersubunit hydrogen bonding was expected to control product distribution by favoring covalent dimer **3** at the expense of higher oligomers. Furthermore, we anticipated that the reversible metathesis reaction would allow depolymerization of undesired higher oligomers and eventual equilibration to the thermodynamic product **3**.[32]

We also explored disulfide bond formation, reasoning that a dimer-forming cyclic peptide bearing two acetamidomethyl cysteine ((Cys(Acm)) residues would undergo covalent capture upon subjection to iodine oxidation (Figure 1). Like olefin metathesis, cysteine oxidation is readily reversible, and for numerous cysteine-rich proteins[37, 38] and protein fragments,[39] oxidative refolding allows conversion of mispaired disulfides to stable native structures. Furthermore, cross-strand disulfides have been shown to reinforce antiparallel β-sheet conformations in natural proteins[40, 41] as well as designed peptides,[42-51] rendering cystine residues attractive tethers for stabilization of cylindrical β-sheet assemblies (Figure 1).

Results

Covalent capture by olefin metathesis: Octapeptide *cyclo*[(-L-Phe-D-^{Me}*N*-Ala-L-Hag-D-^{Me}*N*-Ala)$_2$-] (**1**) bearing two homoallyl side chains was prepared and subjected to ^{1}H NMR, FT-IR, and mass spectral analysis as previously described.[23, 24] The ^{1}H NMR spectrum of **1** was completely assigned from the corresponding ROESY[52] and double quantum-filtered CO-

SY (2QF-COSY)[53] spectra (500 MHz, $CDCl_3$). ROESY experiments revealed three slowly interconverting species, consistent with an equilibrium between monomer **1-m** and the two anticipated dimers, **1-d** and **1-d***. On the basis of variable concentration ^{1}H NMR studies (Figure 2), we found that **1** self-assembles in deuteriochloroform with an overall association constant of $103 \pm 7\ M^{-1}$. The expected antiparallel β-sheet structures of the equally populated dimers **1-d** and **1-d*** were corroborated by solution FT-IR studies of **1** and by analogy to ESI-MS, X-ray crystallographic, and ROE data for related compounds.[23]

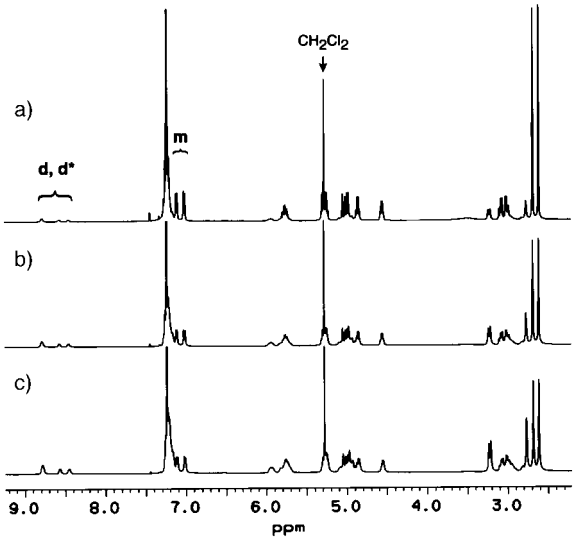

Figure 2. Variable concentration ^{1}H NMR spectra of dimer-forming peptide **1** (500 MHz, 293 K, $CDCl_3$). From top to bottom, spectra are arranged in order of increasing peptide concentration: a) 1.0 mM; b) 3.0 mM; c) 5.0 mM. Due to slow exchange, signals from both monomer (**m**) and the equally populated dimers (**d** and **d***) are observed. As total peptide concentration is raised, the intensities of free N–H resonances arising from **1-m** ($\delta = 7.02$ and 7.12) decrease, while signals corresponding to the equally populated, hydrogen-bonded **1-d** and **1-d*** ($\delta = 8.46 - 8.78$) increase. Other changes are visible in the $C^{\alpha}H$ ($\delta = 4.56 - 5.95$) and N-CH_3 ($\delta = 2.61 - 3.24$) regions.

In a representative metathesis experiment, 26 mol% Ru^{II} catalyst **II** was treated with a deuteriochloroform solution of **1** (5 mM), and the resulting reaction was monitored by analytical RP-HPLC (C18 column). Initially ($\approx 0.5 - 2$ h), consumption of starting material was accompanied by transient buildup of two late-running species, identified by ESI-MS as *E*- and *Z*-mono-metathesized products **2** (hereafter referred to as *intermediates* **2** or *linear dimers* **2**). As the reaction proceeded, new peaks appeared with retention times midway between those of starting compound **1** and intermediates **2**. ^{1}H NMR and ESI-MS analysis identified these species as the expected 38-membered ring-containing tricyclic products **3** present as a mixture of three possible olefin isomers: *E*,*E*; *Z*,*Z*; and *E*,*Z* (Figure 3). Observation of strongly downfield-shifted N–H resonances between 8.07 and 9.01 ppm is consistent with the expected hydrogen-bonded structure.

After two days reaction time, dimeric products **3** were formed in 65% yield as judged by analytical RP-HPLC. While significant quantities of linear dimers **2** remained, we observed no evidence of undesired intramolecular metathesis products or higher oligomers by either RP-HPLC or ESI-MS (Figure 4). The identity of **2** as reaction intermediates was supported by control experiments in which purified samples were resubjected to the original reaction conditions, resulting in formation of di-metathesize products **3**. Thus the covalent capture process appears to proceed in a stepwise fashion, with initial cross-metathesis to yield **2** followed by RCM to give **3** (Figure 5). Control experiments carried out in solvents which abolish intersubunit hydrogen bonding (EtOH or 1:1 v/v DMF/$CHCl_3$) yielded no reaction, underscoring the importance of noncovalent assembly.

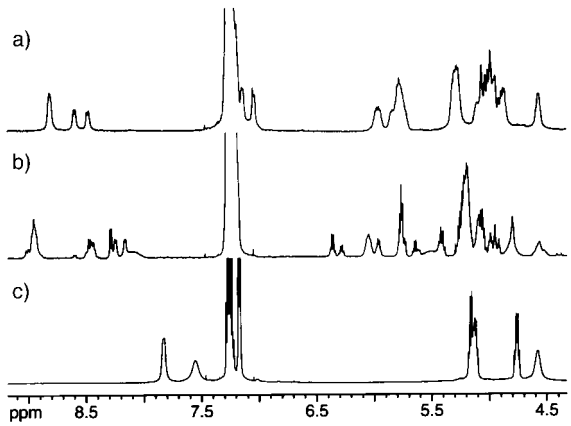

Figure 3. ^{1}H NMR spectra (500 MHz, $CDCl_3$) displaying N–H and $C^{\alpha}H$ resonances of a) olefinic peptide **1** (5.0 mM, 293 K), b) metathesis products **3** (7.1 mM, 293 K), and c) hydrogenated product **4** (4.8 mM, 283 K). Spectrum a) displays resonances for non-hydrogen-bonded N–H groups of Phe and Hag at $\delta = 7.12$ and 7.02, respectively, as well as resonances for hydrogen-bonded N–H groups from two equally populated noncovalent dimers at $\delta = 8.57$ and 8.78 (**1-d**) and $\delta = 8.78$ and 8.46 (**1-d***). Spectrum b) shows resonances for hydrogen-bonded N–H groups between $\delta = 8.07$ and 9.01 and reflects the presence of three olefin isomers (*E*,*E*; *E*,*Z*; and *Z*,*Z*) of **3**. Reduction of **3** produces a single D_2 symmetrical product **4** with signals for the hydrogen-bonded N–H groups at $\delta = 7.56$ (Phe) and 7.83 (Hag) (spectrum c).

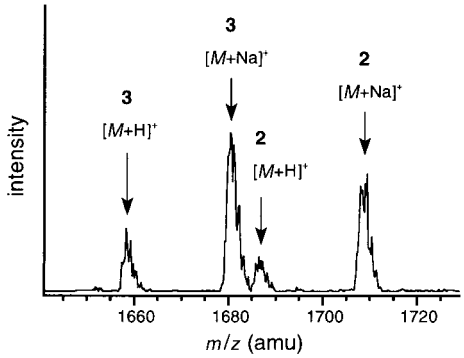

Figure 4. ESI-MS of the crude reaction mixture from olefin metathesis of **1**. Peaks corresponding to singly charged proton and sodium adducts of linear intermediates **2** and tricyclic products **3** appear at 1687, 1709 and 1658, 1680, respectively.

In order to reduce spectral complexity and thereby facilitate ^{1}H NMR characterization, we first hydrogenated **3** in the presence of Pd/C, resulting in quantitative conversion to reduced tricyclic product **4** (Figure 5). Alternatively, the crude

0947-6539/99/0502-0784 $ 17.50+.50/0 *Chem. Eur. J.* **1999**, *5*, No. 2

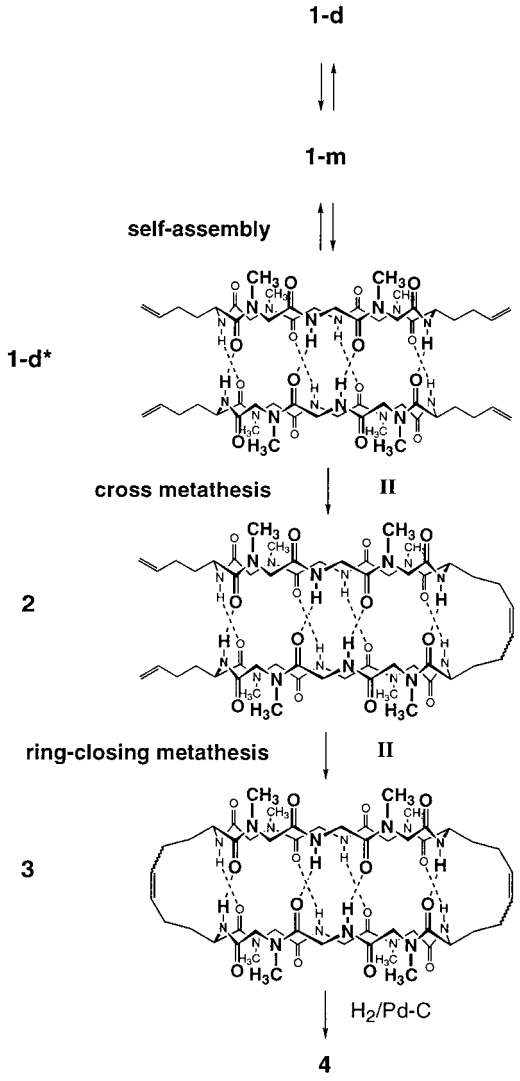

Figure 5. Covalent capture of Hag peptide **1** using Ru^{II} catalyst **II** appears to proceed in a stepwise fashion through the intermediacy of noncovalent dimer **1-d***. The high effective molarity of olefin functions in **1-d*** drives the initial cross metathesis event to give linear intermediates **2**. Compounds **2** then undergo RCM to produce desired products **3**. We then hydrogenated products **3** in order to reduce ^{1}H NMR spectral complexity caused by olefin isomerism, resulting in reduced compound **4**. (For clarity, most side chains are omitted.)

metathesis mixture was first hydrogenated and subsequently purified by RP-HPLC. Compound **4** was subjected to ^{1}H NMR, FT-IR, and ESI mass spectral characterization. The 1D ^{1}H NMR spectrum is consistent with the expected D_2 symmetrical structure and exhibits signals for hydrogen-bonded Phe and Hag N–H groups at 7.56 and 7.83 ppm, respectively (Figure 3). 2D ROESY and COSY experiments established the anticipated covalent and spatial arrangements of atoms in **4** and allowed complete assignment of resonances (Figure 6). Cross-strand $d_{\alpha\text{-}\alpha}$ and $d_{\beta\text{-}\beta}$ ROEs confirmed the expected antiparallel β-sheet topology.[23] Additionally, the solution FT-IR spectrum ($CDCl_3$) closely resembles that of previously characterized dimer-forming peptides, with hydrogen-bonded amide A signals at 3310 cm^{-1} and amide $I_\perp$ bands at 1632 and 1674 cm^{-1}, the latter presumably arising from non-hydrogen-bonding N-alkylated residues.[23]

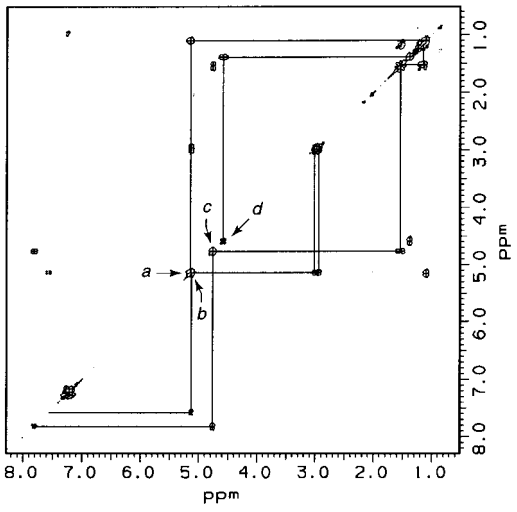

Figure 6. 2QF-COSY spectrum of D_2 symmetrical reduced product **4** (500 MHz, 283 K, $CDCl_3$). C^αH diagonal peaks are labeled as follows: *a*) D-^{Me}*N*-Ala^2 (5.16); *b*) L-Phe^1 (5.12); *c*) L-Hag^3 (4.76); *d*) D-^{Me}*N*-Ala^4 (4.59).

Covalent capture by disulfide formation. Peptide *cyclo*[(-L-Phe-D-^{Me}*N*-Ala-L-Cys(Acm)-D-^{Me}*N*-Ala)$_2$-] (**5-Acm**) was synthesized by standard protocols and characterized by ^{1}H NMR spectroscopy and ESI mass spectrometry (see Experimental Section). Surprisingly, ^{1}H NMR experiments revealed that **5-Acm** exists in deuteriochloroform solely as a monomer. Nevertheless, by analogy to metathesis experiments described above, we reasoned that the conformationally rigid peptide ring would favor inter- over intramolecular disulfide formation, thereby enforcing hydrogen bonding and subsequent oxidative ring closure. The slow rate of Cys(Acm) oxidation in nonpolar solvents required us to carry out the reaction in aqueous media.[54] Under these conditions, however, iodine oxidation of **5-Acm** yielded exclusively monomeric cystine peptide **5-SS** (Figure 7).

Next we considered oxidative capture of the free sulfhydryl derivative. Upon reduction of disulfide **5-SS**, the resulting dithiol **5-SH** also exhibited no evidence of self-association. We then decided to pursue a different strategy. By analogy to mercaptan-catalyzed 'unscrambling' of mispaired disulfides in proteins such as bovine pancreatic ribonuclease A (RNase A),[38] we reasoned that in the presence of a sulfhydryl reagent, the half-cystine residues of **5-SS** would rearrange by thiol–disulfide interchange to produce target dimer **7**. We predicted that release of conformational strain in **5-SS** and the potential for intersubunit hydrogen bonding together with the entropic drive toward maximizing the number of particles in solution would favor the desired product **7** at the expense of both monomer **5-SS** and alternative higher oligomers.

This strategy proved successful. In a typical experiment, we treated 10–29 mol% dithiol **5-SH** with a solution of substrate **5-SS** (5–6 mM, $CHCl_3$) followed by 1% v/v Et_3N, and monitored the resulting reaction by RP-HPLC (C4 column). Initially (0.5–24 h), the appearance of numerous late running species accompanied consumption of **5-SS** (Figure 8). We isolated these compounds and identified them as linear dimeric, trimeric, tetrameric, and pentameric disulfide-bonded oligomers (compounds **6**) using matrix-assisted laser

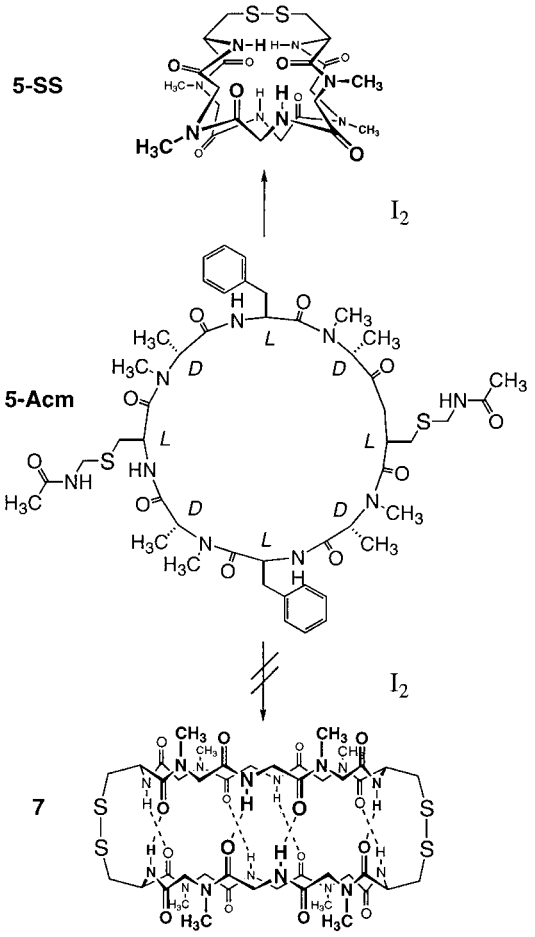

Figure 7. Iodine oxidation of di-Cys(Acm) peptide **5-Acm** gave cystine-containing monomer **5-SS** rather than expected disulfide-bonded dimer **7**. (For clarity, most side chains are omitted.)

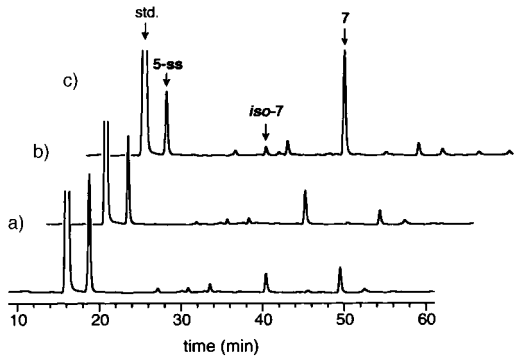

Figure 8. Time dependence of the analytical RP-HPLC profile for disulfide isomerization of **5-SS** catalyzed by **5-SH** ($\lambda = 230$ nm): a) 6 h; b) 16 h; c) 48 h. Peaks arising from internal standard 9-fluorenone, starting material **5-SS**, isomeric dimer *iso*-**7**, and desired disulfide-bonded dimer **7** are indicated. Unlabeled peaks corresponding to linear dimeric, trimeric, tertrameric, and pentameric products **6** appear at approximately 34, 49, 53, and 56 minutes, respectively. As the reaction proceeds, target product **7** begins to predominate at the expense of **5-SS** and intermediates **6** and *iso*-**7**. (Data are normalized and baseline corrected.)

desorption ionization mass spectrometry (MALDI-MS, Table 1); smaller peaks presumably arising from higher oligomers were also observed. Upon further reaction, the intensities of oligomeric products **6** decreased with a corresponding increase in the amount of target product **7**. The reaction

Table 1. Species identified by MALDI-MS in the disulfide isomerization of **5-SS**.

Compound	$[M+X]^+$ calcd	$[M+X]^+$ found	X
iso-**7**	1679	1678	H
di-**6**	1681	1679	H
7	1679	1678	H
tri-**6**	2520	2519	H
tetra-**6**	3359	3356	H
penta-**6**	4235	4236	K

generally failed to achieve quantitative consumption of either starting peptide **5-SS** or oligomeric intermediates **6**, likely due to slow oxidation of the dithiol catalyst. However, covalent dimer **7** was typically formed in 50–90% yield after 2–5 days reaction time, with larger amounts of catalyst **5-SH** giving rise to higher yields.

Control experiments provided further insight into the isomerization process. In addition to **5-SH**, we found that sulfhydryl reagents such as 2-mercaptoethanol and thiophenol also catalyzed the reaction. Experiments carried out in the absence of added thiol yielded only starting material even after extended reaction times ($\approx$5 days). Moreover, attempts to regenerate cystine monomer **5-SS** by oxidation of **5-SH** (1 mM in 5:4:1 v/v/v MeOH:H_2O:DMSO; room temperature)[55] proved unsuccessful, supporting the existence of conformational strain in the former. On the basis of these data, the following mechanistic picture emerges. In the minimal catalytic cycle (Figure 9), the reaction begins with intermolecular thiol–disulfide interchange between catalyst **5-SH** and cystine peptide **5-SS**, generating linear oligomer **6**. Compound **6** can then undergo intramolecular disulfide exchange to generate tricyclic product **7** as well as a new linear oligomer **6** shortened by two cyclic peptide subunits. Additional rounds of inter- and intramolecular exchange occur until thermodynamic product **7** predominates at equilibrium.

During the course of these experiments, we consistently observed a product (*iso*-**7**) whose mass spectrum is identical with that of **7** but which elutes significantly earlier during RP-HPLC analysis (Table 1; Figure 8). On the basis of its apparent hydrophilicity, we tentatively identified *iso*-**7** as the 'inside-out' topological isomer of desired product **7**, with apolar N-methyl groups sandwiched at the dimeric interface and N–H moieties pointing outward toward the surrounding medium (Figure 10). As the reaction proceeds, the intensity of this species diminishes while that of **7** increases, suggesting that *iso*-**7** is a kinetic product which eventually rearranges to give the more stable hydrogen-bonded dimer **7**. Indeed, control experiments carried out in 2.5:1 v/v dimethylacetamide (DMA):$CHCl_3$ yield approximately equimolar amounts of **7** and *iso*-**7**. These data indicate that, while entropic factors apparently favor dimeric products, solvent polarity controls partitioning between hydrogen-bonded **7** and non-hydrogen bonded *iso*-**7**.

UV/Vis and ^{1}H NMR spectroscopy confirmed the anticipated covalent and topological features of peptide **7**. Treatment of a solution of **7** in chloroform with one equivalent of sulfhydryl indicator 2,2′-dipyridyldisulfide[56, 57] yielded no reaction as judged by UV/Vis, demonstrating the absence of

0947-6539/99/0502-0786 $ 17.50+.50/0 *Chem. Eur. J.* **1999**, *5*, No. 2

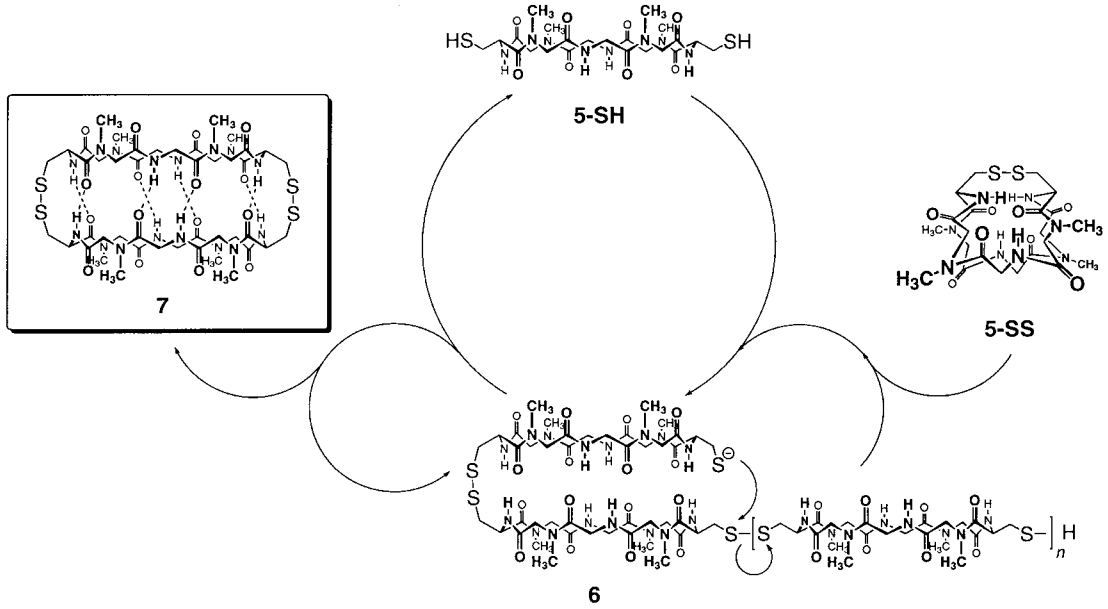

Figure 9. Minimal mechanism for rearrangement of cystine monomer **5-SS** catalyzed by **5-SH**. Cystine monomer **5-SS** first experiences intermolecular thiol–disulfide interchange to give linear oligomer **6**. When $n \geq 1$, **6** can then undergo *intramolecular* exchange to form one equivalent of tricyclic dimer **7** and a new linear oligomer shortened by two cyclic peptide subunits. At this point oligomer **6** can either add to additional equivalents of monomer **5-SS** or undergo further intramolecular exchange to produce **7**, ultimately regenerating catalyst **5-SH**. (For clarity, most side chains are omitted.)

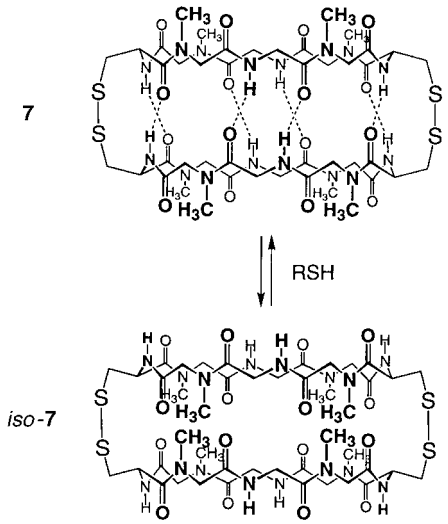

Figure 10. Hydrogen-bonded dimer **7** and putative non-hydrogen-bonded dimer *iso*-**7** can in principle interconvert by thiol–disulfide interchange. In nonpolar solvents **7** predominates, presumably due to stabilization by intramolecular hydrogen bonding, while control experiments carried out in polar solvent mixtures which compete for hydrogen-bonding sites yield approximately equimolar mixtures of the two compounds. (For clarity, most side chains are omitted.)

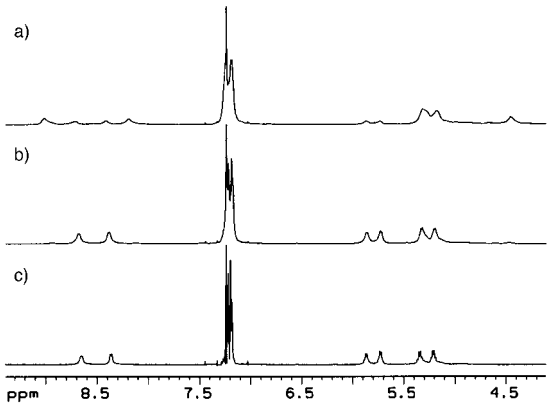

Figure 11. Variable temperature ^{1}H NMR spectra of disulfide-bonded dimer **7** at a) 293 K, b) 308 K, and c) 323 K (500 MHz, $CDCl_3$). Spectrum a shows two sets of signals which begin to converge as the temperature is raised, suggesting the presence of interconverting cystine side chain conformers.

free thiols and affirming the expected disulfide-bonded structure. In variable temperature ^{1}H NMR experiments, **7** shows two sets of signals at room temperature which converge near 323 K (Figure 11), possibly due to interconverting cystine side chain conformers. Downfield-shifted N–H resonances between $\delta = 8.21$ and 9.05 reveal strong intramolecular hydrogen bonding (Figures 11 and 12) and support the proposed role of noncovalent interactions in controlling product distribution (Figure 10). Finally, downfield shifts in $C^{\alpha}H$ signals with respect to both **5-SS** and **5-SH** (Figure 12) together with observation of strong cross-strand $d_{\alpha\text{-}\alpha}$ and intense sequential $d_{\alpha\text{-}N}$ $(i, i+1)$ ROEs established the expected antiparallel β-sheet structure of **7** (Figure 13).[23]

Discussion

Olefin metathesis: The covalent capture strategy outlined in Figure 1 proved successful for olefin metathesis of Hag-bearing peptide **1**, furnishing 38-membered ring-containing tricyclic products **3** in 65% yield. Several lines of evidence establish the importance of noncovalent assembly. ^{1}H NMR experiments demonstrated that starting peptide **1** dimerizes in deuteriochloroform through intersubunit hydrogen bonding with an overall association constant of $103 \pm 7\ \text{M}^{-1}$, while polar solvents such as dimethylformamide (DMF) completely

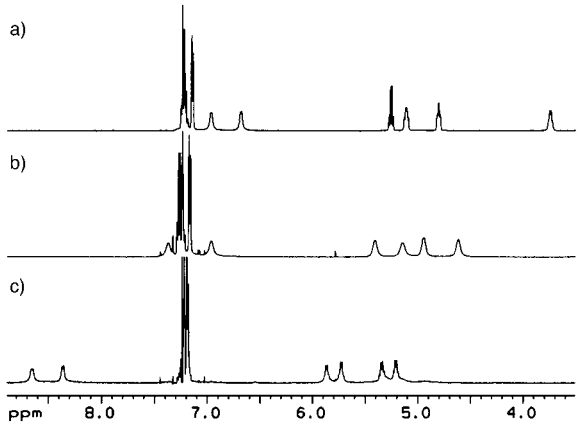

Figure 12. ^{1}H NMR spectra of a) reduced peptide **5-SH** and b) cystine monomer **5-SS** in comparison with that of c) disulfide-bonded dimer **7** (500 MHz, 323 K, $CDCl_3$). Spectrum c shows large downfield shifts in N–H and C$^\alpha$H resonances with respect to spectra a and b, demonstrating strong intramolecular hydrogen bonding and β-sheet structure, respectively, in **7**.[23]

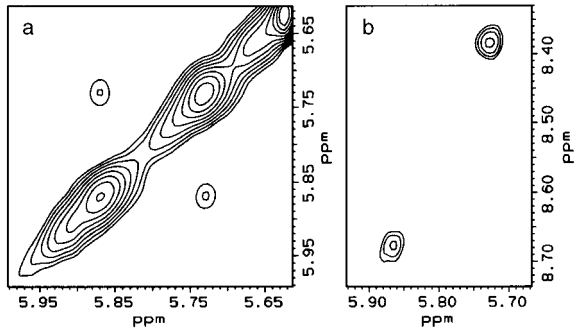

Figure 13. ROESY spectrum of disulfide-bonded dimer **7**, showing a) strong cross-strand Ala^4 to Ala^2 $d_{\alpha\text{-}\alpha}$ and b) intense $d_{\alpha\text{-N}}$ $(i, i+1)$ ROEs characteristic of antiparallel β-sheet structure.[23] In spectrum b, intraresidue $d_{\alpha\text{-N}}$ ROE crosspeaks are expected to be weaker than the corresponding sequential signals shown here and were not observed in this experiment.

abolish self-assembly. Thus we predicted that nonpolar solvents would favor covalent capture by promoting hydrogen bonding and thereby increasing olefin effective molarity. Indeed, the reaction proceeded smoothly in deuteriochloroform, while control experiments carried out in polar media (EtOH or 1:1 v/v DMF:$CHCl_3$) yielded no metathesis products. Furthermore, although polar solvents are known to reduce the activity of Ru^{II} complex **II**, Grubbs et al. have successfully utilized this catalyst to effect cross metathesis of *cis*-2-pentene in both [D_8]THF and 0.29:1 v/v MeOD:CD_2Cl_2 ([substrate] = 0.606 M and 0.519 M, respectively).[31] These data indicate that, in the absence of noncovalent dimer formation, metathesis of **1** does not occur at an appreciable rate under the dilute conditions employed ($\approx$5 mM). Consistent with this explanation, high dilution ($\leq \approx$20 mM) is known to suppress acyclic olefin cross metathesis in other substrates.[32] Therefore the appearance of metathesis products in the present system supports the importance of noncovalent assembly.

During the course of the reaction we noticed transient buildup of mono-metathesized intermediates **2**, indicating that the second step (ring closure) occurs at a rate comparable to the first (cross metathesis). These observations suggest that both metathesis events take place in an *intramolecular* fashion, in agreement with the proposed covalent capture mechanism (Figure 5). Furthermore, no ring-closing metathesis of **1** was detected, presumably due to rigidity of the peptide ring.

Target products **3** were characterized by analytical RP-HPLC, ESI-MS, and ^{1}H NMR spectroscopy. As expected, **3** exists as a mixture of three olefin isomers (*E*,*E*; *E*,*Z*; and *Z*,*Z*). Downfield shifted N–H signals between $\delta = 8.07$ and 9.01 strongly support the expected hydrogen-bonded structure (Figure 3b). Following hydrogenation of olefin functionalities, N–H and C$^\alpha$H resonances of reduced product **4** experience upfield shifts with respect to both metathesis products **3** and noncovalent dimers **1-d** and **1-d*** (Figure 3). These shifts demonstrate weaker hydrogen bonding and a lesser degree of β-sheet structure in **4**, likely reflecting unfavorable steric constraints imposed by saturated Hag linker groups. Nevertheless, observation of cross-strand $d_{\alpha\text{-}\alpha}$ and $d_{\beta\text{-}\beta}$ ROEs together with solution FT-IR data identify the overall topology of **4** as that of an antiparallel β-sheet.[23]

Our preliminary account of this work represents the first example of acyclic olefin cross metathesis promoted by noncovalent assembly.[24] Previously, Grubbs et al. had employed intramolecular hydrogen bonding to organize olefin-bearing peptides for RCM.[33, 58] Subsequent studies have exploited a more reactive third-generation Ru^{II} catalyst to effect template-directed cyclization,[32] catenation,[59] and knot-formation.[60] Finally, a recent report from Grubbs et al. described RCM of preorganized α-helical peptides bearing olefinic residues at i and $i+4$ positions.[61] The present study therefore compliments ongoing efforts to define the scope and limitations of olefin metathesis in self-assembling and self-organizing systems.

Disulfide bond formation: We also employed intersubunit hydrogen bonding to effect selective conversion of di-Cys(Acm)-containing peptide **5-Acm** to disulfide-bonded dimer **7** (Figures 7 and 9). Since both **5-Acm** and deprotected derivative **5-SH** failed to self-associate in deuteriochloroform, we were unable to apply the general strategy outlined in Figure 1. This lack of self-association was unexpected and may arise from intramolecular hydrogen bonding. Consistent with this interpretation, we recently found that related peptides with general sequence *cyclo*[(-L-Phe-D-^{Me}*N*-Ala)$_3$-L-Xaa-D-^{Me}*N*-Ala-] dimerize only weakly ($K_a < \approx 5\,M^{-1}$ in $CDCl_3$), if at all, when Xaa is a polar residue such as Ser or Orn.[62] We therefore obtained **7** indirectly from **5-Acm** through a two-step procedure involving intramolecular oxidation (Figure 7) followed by hydrogen-bond-directed thiol-catalyzed isomerization (Figure 9).

Several observations provided mechanistic insight into the disulfide isomerization process. The reaction proceeded smoothly in the presence of catalytic amounts of sulfhydryl compounds including **5-SH**, thiophenol**,** and 2-mercaptoethanol (5–6 mM in **5-SS**, 1% v/v Et_3N, $CHCl_3$), while the omission of thiol furnished only starting material. Upon increasing the amount of catalyst **5-SH** from 10 to 29 mol%, we found that the yield of **7** rose from 50 to 90% with a corresponding increase in consumption of both **5-SS** and oligomeric intermediates **6**. This observation suggests that, as expected, the

0947-6539/99/0502-0788 $ 17.50+.50/0 *Chem. Eur. J.* **1999**, *5*, No. 2

thiol–disulfide interchange reaction is inhibited by slow oxidation of both **5-SH** and **6**. Furthermore, unlike the metathesis system discussed above, the covalent capture process leading to disulfide-bonded dimer **7** *necessarily* involves oligomeric intermediates. These oligomers must be at least three cyclic peptide subunits in length: two undergo thiol–disulfide interchange, while the third acts as a leaving group (Figure 9). Higher oligomers likely result from competition between intra- and intermolecular exchange under initial conditions when the concentration of **5-SS** is highest. Thus observation of oligomeric intermediates in the disulfide isomerization of **5-SS** strongly supports our proposed mechanism.

Conformational strain appears to activate the disulfide bond in **5-SS** for initial nucleophilic attack by **5-SH**. In support of this hypothesis, monomeric cystine peptide **5-SS** is readily converted to alternative disulfide-bonded species in the presence of catalytic amounts of thiol (Figure 8). Furthermore, dithiols typically exhibit high oxidation potentials arising from proximity effects.[63] For example, we have found that the related peptide *cyclo*[(-D-Phe-L-*N*-(*n*-propanethiol)-Ala-D-Phe-L-Ala)$_2$-] undergoes facile and quantitative air oxidation to give the corresponding intramolecular disulfide.[64] In contrast, attempts to regenerate **5-SS** by DMSO oxidation of **5-SH** (1 mM in 5:4:1 v/v/v MeOH:H_2O:DMSO; room temperature)[55] were unsuccessful, providing additional evidence of conformational strain.

The data indicate that hydrogen bonding plays an important role in controlling product distribution. For example, the hydrogen bonding observed in ^{1}H NMR spectra of **7** likely contributes to the stability of this compound and should therefore favor its formation (Figure 12). Furthermore, control experiments carried out in a polar solvent mixture which disfavors hydrogen bonding (2.5:1 v/v DMA:$CHCl_3$) yielded predominantly an equimolar mixture of dimeric products **7** and *iso*-**7**. On the basis of ESI-MS and analytical RP-HPLC data, we identified *iso*-**7** as the 'inside-out' topological isomer of target product **7** (Table 1; Figures 8 and 10). Under the usual reaction conditions ($CHCl_3$), *iso*-**7** is apparently formed as an intermediate but then reverts to the more stable hydrogen-bonded structure **7**. These observations strongly suggest that entropic factors favor dimeric products regardless of solvent polarity, while in nonpolar media **7** predominates due to intramolecular hydrogen bonding.

The unreactivity of **7** toward 2,2′-dithiodipyridine[56, 57] demonstrated the absence of free sulfhydryl groups and established the expected disulfide-bonded structure. Additionally, ROESY experiments allowed complete assignment of ^{1}H NMR resonances and affirmed the expected antiparallel β-sheet structure. In contrast to **7**, most other disulfide-tethered β-sheet model systems contain cystine residues at non-hydrogen-bonding positions.[42-49] However, numerous examples of cyclic tetrapeptide β-turn mimetics incorporating cysteine disulfides at hydrogen-bonding i and $i+4$ positions provide ample precedent for the arrangement of residues in **7**.[50, 51] Indeed, downfield shifts in N–H and C$^\alpha$H resonances with respect to both **5-SS** and **5-SH** (Figure 12) as well as strong cross-strand $d_{\alpha\text{-}\alpha}$ and intense sequential $d_{\alpha\text{-N}}$ (i, $i+1$) ROEs (Figure 13) distinctly resemble ^{1}H NMR features of noncovalent cylindrical β-sheet peptide assemblies.[23] Furthermore, N–H and C$^\alpha$H signals of **7** exhibit larger downfield shifts than corresponding resonances in reduced metathesis product **4**, indicating that cystine residues are better suited for tethering adjacent cyclic peptide subunits.

Observation of two sets of signals in ^{1}H NMR spectra of **7** strongly suggests the presence of interconverting cystine side chain conformers. Like other alkyldisulfides, cystine residues typically exhibit equilibrium χ_{ss} values restricted to the ranges $90 \pm 20^\circ$ (p) and $-90 \pm 20^\circ$ (n)[41] as well as twofold rotational barriers at 0° (*cis*) and 180° (*trans*).[65, 66] To a first approximation, these features can be visualized as arising from lone pair repulsion between adjacent sulfur atoms.[65, 66] In the absence of impediments such as cyclization or steric interactions, interconversion between p and n forms is expected to occur through the *trans* pathway due to the higher activation barrier for *cis* rotation (≈ 11 kcal mol^{-1} for *cis* vs. ≈ 5–6 kcal mol^{-1} for *trans*).[67] As with other cyclic systems, however, conformational constraints in **7** could force χ_{ss} rotation through the less stable *cis* rotamer.[67] Transient breakage of up to eight intramolecular hydrogen bonds may further increase this activation barrier, giving rise to slow exchange observed in ^{1}H NMR spectra of **7** (Figure 11).

The present study adds to a growing number of investigations into the use of disulfides to stabilize self-assembling and self-organizing systems. Well known examples include the aforementioned oxidative refolding of natural cysteine-rich proteins[37, 38] and protein fragments.[39] In addition, chemists have employed disulfides to covalently capture preorganized single α-helical[68] and coiled-coil peptides,[69, 70] as well as nucleic acid[71, 72] and lipid assemblies.[73] The chemoselectivity and ready reversibility of disulfide formation render this transformation especially well suited to stabilization of delicate constructs.

Conclusion

We have successfully employed hydrogen bonding to organize cyclic peptide subunits for intermolecular covalent bond formation, resulting in kinetically stable cylindrical β-sheet assemblies. In the two systems explored, we found that hydrogen bonding plays different yet equally important roles. For olefin metathesis of peptide **1**, hydrogen bonding apparently drives covalent bond formation by increasing olefin effective molarity, as evidenced by the lack of reaction in polar media which disfavor the assembly process. In contrast, release of conformational strain provides the driving force for thiol–disulfide interchange of **5-SS**, furnishing entropically favored dimeric products in both polar and nonpolar solvents. In this case, however, hydrogen bonding in nonpolar media appears to control product distribution by stabilizing dimer **7** and favoring its production at the expense of non-hydrogen-bonded *iso*-**7**.

Both olefin metathesis of **1** and oxidation of **5-Acm** lead to products displaying the expected antiparallel β-sheet hydrogen-bonding network, indicating that the tethers employed are suitable for bridging adjacent cyclic peptide subunits. However, hydrogenation of olefin groups in metathesis

products **3** causes weaker hydrogen bonding and a lesser degree of β-structure in reduced product **4**, suggesting unfavorable conformational restraints imposed by the saturated linker groups. These observations will aid in design of novel functional materials based on covalently polymerized cyclic peptide nanotubes.

Experimental Section

Chemicals: Acetonitrile, isopropyl alcohol (optima, Fisher), and trifluoroacetic acid (Halocarbon, NJ) for analytical RP-HPLC were used without further purification. Chloroform (optima, Fisher) was dried and deoxygenated prior to use by distillation from $CaCl_2$ under argon. Dimethylacetamide was purified by vacuum distillation from ninhydrin, dried over 8–12 mesh 4 Å molecular sieves, and deoxygenated by sparging with argon before use. Dimethylformamide (DMF, sequencing grade, Fisher) and ethanol for metathesis experiments were deoxygenated by sparging with argon before use. Thiophenol, 2-mercaptoethanol, 9-fluorenone, 2,2′-dipyridyldisulfide, hexafluoroisopropanol (HFIP), heptafluorobutyric acid (HFBA), and hexafluoroacetone hydrate (HFA $\cdot x\,H_2O$), and anhydrous dioxane were used as obtained from Aldrich. Dithiothreitol (DTT) was purchased from Fisher and used without further purification. Triethylamine was obtained from Fisher and distilled first from ninhydrin and then from CaH_2 under Ar and stored over KOH pellets. $CDCl_3$ (99.8%, Isotech) for ^{1}H NMR spectroscopy and metathesis experiments was distilled from $CaCl_2$ under Ar prior to use.

Peptide synthesis and cyclization: Except as noted, peptide synthesis and cyclization was carried out as previously described.[23] Details concerning the synthesis and characterization of *cyclo*[(-L-Phe-D-^{Me}*N*-Ala-L-Hag-D-^{Me}*N*-Ala)$_2$-] (**1**) are reported elsewhere.[23]

***cyclo*[(-L-Phe^1-D-^{Me}*N*-Ala^2-L-Cys(Acm)^3-D-^{Me}*N*-Ala^4)$_2$-] (5-Acm)**: Linear octapeptide [(-L-Phe-D-^{Me}*N*-Ala-L-Cys(Acm)-D-^{Me}*N*-Ala)$_2$ (**5-x**) was synthesized on *N*-Boc-D-^{Me}*N*-Ala-(OCH$_2$)-Pam resin (1.31 mmol scale). After introduction of the first Cys(Acm) residue, the peptidyl resin was scrupulously washed with CH_2Cl_2 before and after each TFA treatment in order to minimize side reactions arising from exothermic reaction of TFA with DMF. After HF cleavage and purification by RP-HPLC, desired product **5-x** was obtained as its TFA salt in 75% yield (1.095 g, 982 μmol; ESI-MS: $[M+H]^+$ calcd 1001.5; found 1001). Cyclization of **5-x** (500 mg, 449 μmol) followed by RP-HPLC purification afforded **5-Acm** in 67% yield (255 mg, 303 μmol). ^{1}H NMR (500 MHz, 323 K, $CDCl_3$): **L-Phe^1**: $\delta =$ 7.00 (br, N–H), 4.96 (m, C$^\alpha$H), 2.91, 2.94, (m, C$^\beta$H$_2$), 7.12–7.34 (m, C$^{\delta,\varepsilon,\xi}$H); **D-^{Me}*N*-Ala^2**: $\delta = 2.77$ (s, N–CH$_3$), 5.45 (br, C$^\alpha$H), 1.22 (br s, C$^\beta$H$_3$); **L-Cys(Acm)^3**: $\delta = 7.41$ (br, N–H), 4.86 (m, C$^\alpha$H), 2.83, 3.10 (m, C$^\beta$H$_2$), 4.38 (m, Acm CH$_2$), 6.99 (br, Acm N–H), 2.04 (s, Acm CH$_3$); **D-^{Me}*N*-Ala^4**: $\delta =$ 2.77 (s, N–CH$_3$), 5.16 (br, C$^\alpha$H), 1.26 (br s, C$^\beta$H$_3$); ESI-MS: $[M+H]^+$ calcd 983.4; found 983.

***S*,*S*′-dithio-(*cyclo*[(-L-Phe^1-D-^{Me}*N*-Ala^2-L-Cys^3-D-^{Me}*N*-Ala^4)$_2$-]) (5-SS)**: To a 50 mL round-bottom flask equipped with magnetic stir bar was added one equivalent of di-Cys(Acm)-containing cyclic octapeptide **5-Acm** (100 mg, 102 μmol) followed by 60:40 v/v acetic acid:water containing one equivalent of I_2 (20.0 mL, 5.10 mM, 102 μmol).[54] The resulting reaction mixture was stirred at 50 °C for 12 h, at which time excess I_2 was reduced by addition of 10% aqueous $Na_2S_2O_3$ (40 μL). The solution was subjected directly to RP-HPLC to give the desired cystine-containing heterodectic bicyclic octapeptide **5-SS** in 47% yield (40 mg, 48 μmol). ^{1}H NMR (500 MHz, 323 K, $CDCl_3$): **L-Phe^1** : $\delta = 6.70$ (br s, N–H), 5.13 (m, C$^\alpha$H), 2.93, 3.13 (m, C$^\beta$H$_2$), 7.14–7.28 (m, C$^{\delta,\varepsilon,\xi}$H); **D-^{Me}*N*-Ala^2**: $\delta = 2.45$ (s, N–CH$_3$), 5.31 (q, $J =$ 6.8 Hz, C$^\alpha$H), 1.09 (d, $J = 6.8$ Hz, C$^\beta$H$_3$); **L-(dithio)-Cys^3**: $\delta = 6.99$ (br, N–H), 4.83 (m, C$^\alpha$H), 2.98, 3.32 (m, C$^\beta$H$_2$); **D-^{Me}*N*-Ala^4**: $\delta = 3.12$ (s, N–CH$_3$), 3.80 (br, C$^\alpha$H), 1.40 (d, $J = 6.8$ Hz, C$^\beta$H$_3$); ESI-MS: $[M+H]^+$ calcd 839.4; found 839.

***cyclo*[(-L-Phe^1-D-^{Me}*N*-Ala^2-L-Cys^3-D-^{Me}*N*-Ala^4)$_2$-] (5-SH)**: A 25 mL round-bottom flask equipped with magnetic stir bar was charged with one equivalent of cystine-containing bicyclic octapeptide **5-SS** (20 mg, 24 mmol), 50 equivalents of DTT (184 mg, 1.2 mmol), and $CHCl_3$ (10 mL). Five equivalents of Et_3N were then added (21 μL, 120 μmol), and the resulting mixture was stirred 12 h at room temperature under N_2. The reaction was terminated by washing with saturated NH_4Cl (1×5 mL) and brine (1×5 mL), followed by drying with Na_2SO_4. After removal of the solvent under reduced pressure, the crude product was transferred neat to a 1.5 mL microcentrifuge tube, to which was added H_2O (1 mL). The tube was then vortexed briefly and centrifuged to effect solid/liquid separation. After decanting the supernatant, the solid was washed twice more in this fashion, then purified by RP-HPLC to give reduced product **5-SH** in 96% yield (19.5 mg, 23 μmol). ^{1}H NMR (400 MHz, 293 K, $CDCl_3$): **L-Phe^1**: $\delta = 7.04$ (br, N–H), 4.90 (m, C$^\alpha$H), 2.92, 2.94 (m, C$^\beta$H$_2$), 7.17–7.28 (m, C$^{\delta,\varepsilon,\xi}$H); **D-^{Me}*N*-Ala^2**: $\delta = 2.73$ (br s, N–CH$_3$), 5.42 (br, C$^\alpha$H), 1.18 (br s, C$^\beta$H$_3$); **L-Cys^3**: $\delta = 7.55$ (br, N–H), 4.53 (m, C$^\alpha$H), 2.71, 3.03 (m, C$^\beta$H$_2$), 1.66 (br, SH); **D-^{Me}*N*-Ala^4**: $\delta = 2.72$ (br s, N–CH$_3$), 5.15 (br, C$^\alpha$H), 1.24 (br s, C$^\beta$H$_3$); ESI-MS: $[M+H]^+$ calcd 841.4; found 841.

Metathesis experiments with olefin-bearing peptide 1: Experiments were typically carried out according to the following representative procedure. Under argon, HPLC-purified olefinic peptide **1** (≈8 mg, ≈9 mmol) was dissolved in dry, deoxygenated $CDCl_3$ (≈0.6 mL) and allowed to sit for 30 min over freshly activated 8–12 mesh 4 Å molecular sieves (≈100 mg). An aliquot (150 μL) was then withdrawn and diluted with $CDCl_3$ (300 μL) and a 1.0% stock solution of anhydrous dioxane in $CDCl_3$ (50 μL). The ^{1}H NMR spectrum of this sample was acquired, and from the integral ratio of dioxane to total C$^\alpha$H and olefinic protons, the stock solution was determined to be 8.36 mM in **1**. The remaining stock solution was recovered (480 μL, 4.0 mmol) and diluted with $CDCl_3$ (800 μL total volume, 5.0 mM in **1**). 26 mol% Ru^{II} metathesis catalyst **II** was then added (0.95 mg, 1.03 μmol), and the resulting reaction mixture was monitored by analytical RP-HPLC (C_{18} column/*i*PrOH/H_2O). After two days, an aliquot was removed and analyzed. A stock solution of **1** (2.5 mM) was then coinjected with the crude reaction mixture to provide an internal standard. By coinjecting standard solutions of **3** and **1**, we had previously found the ratio of ε_{230} to be 2.0. After subtracting the intensity of residual starting material, we determined that products **3** had been formed in 65% yield. Linear dimers **2** were purified by RP-HPLC and identified by mass spectral methods (ESI-MS: $[M+H]^+$ calcd 1687; found 1687). Target products **3** were isolated and characterized by ^{1}H NMR spectroscopy (Figure 3b) and mass spectrometry (ESI-MS: $[M+H]^+$ calcd 1659; found 1658). Hydrogenation of **3** in the presence of 1 wt equivalent 10% Pd-C (1 atm H_2) afforded reduced product **4** in essentially quantitative yield. ^{1}H NMR (500 MHz, 283 K, $CDCl_3$): **L-Phe^1**: $\delta = 7.56$ (br, N–H), 5.12 (m, C$^\alpha$H), 2.92–3.04 (m, C$^\beta$H$_2$), 7.16–7.29 (m, C$^{\delta,\gamma,\varepsilon}$H); **D-^{Me}*N*-Ala^2**: $\delta =$ 2.48 (s, N–CH$_3$), 5.16 (q, $J = 7.0$ Hz, C$^\alpha$H), 1.09 (d, $J = 7.0$ Hz, C$^\beta$H$_3$); **L-Hag^3**: $\delta = 7.83$ (d, $J = 7.6$ Hz, N–H), 4.76 (m, C$^\alpha$H), 1.54 (m, C$^\beta$H$_2$), 1.18–1.26 (m, C$^{\gamma,\delta}$H$_2$); **D-^{Me}*N*-Ala^4**: $\delta = 3.06$ (s, N–CH$_3$), 4.59 (br, C$^\alpha$H), 1.40 (d, $J = 7.3$ Hz, C$^\beta$H$_3$); ESI-MS: $[M+H]^+$ calcd 1663; found 1662.

Disulfide isomerization of cystine monomer 5-SS: The reaction was typically carried out according to the following representative procedure. Lyopholized peptide **5-SS** (≈2.5 mg) was placed in a 1 mL Schlenk tube and purged with argon. A stock solution of 9-fluorenone (30.5 mM, 100 μL) was added as an internal standard, followed by Et_3N (5 μL, 1% v/v). The reaction was initiated by addition of a stock solution of dithiol compound **5-SH** (100 μL, ≈10 mol% relative to **5-SS**), then quickly increasing the total volume to 500 μL. An aliquot was then withdrawn (10 μL) and diluted with of 9:1 v/v HFIP/HFBA (60 μL) followed by HFA $\cdot 3\,H_2O$ (250 μL). By analytical RP-HPLC we determined that [**5-SS**] = 4.7 M. The reaction was left sealed for 12 days under argon, after which time analytical RP-HPLC revealed a 50% yield of disulfide-bonded dimer **7**. ^{1}H NMR (500 MHz, 313 K, $CDCl_3$): **L-Phe^1**: $\delta = 8.68$ (br, N–H), 5.33 (m, C$^\alpha$H), 2.70–3.30 (m, C$^\beta$H$_2$), 7.16–7.28 (m, C$^{\delta,\gamma,\varepsilon}$H); **D-^{Me}*N*-Ala^2**: $\delta = 2.80$ (s, N-CH$_3$), 5.73 (br, C$^\alpha$H), 1.01 (br s, C$^\beta$H$_3$); **L-(dithio)-Cys^3**: $\delta = 8.39$ (br, N–H),5.21 (m, C$^\alpha$H), 2.70–3.30 (m, C$^\beta$H$_2$); **D-^{Me}*N*-Ala^4**: $\delta = 3.29$ (s, N-CH$_3$), 5.87 (m, C$^\alpha$H), 1.21 (br s, C$^\beta$H$_3$); ESI-MS ($[M+H]^+$ calcd 1679, found 1678).

^{1}H NMR characterization of compounds: ^{1}H NMR spectra ($CDCl_3$) of compounds **4**, **5-Acm**, **5-SS**, **5-SH**, and **7** were assigned from the corresponding ROESY[52] and/or double quantum-filtered 2D COSY (2QF-COSY)[53] spectra. Characterization of peptide **1** has been previously described.[23] Mixing times (≈300 ms) were not optimized for ROESY experiments. Due to conformational averaging at the temperature indicated, ^{1}H NMR spectra of peptides **5-Acm**, **5-SS**, and **5-SH** were C_2 symmetrical, while those of **4** and **7** displayed D_2 symmetry. Spectra were typically acquired using Bruker's standard pulse sequence on an AMX-400

0947-6539/99/0502-0790 $ 17.50+.50/0 *Chem. Eur. J.* **1999**, *5*, No. 2

or 500 MHz spectrometer as indicated for each compound and referenced to residual $CHCl_3$ solvent peaks ($\delta = 7.24$). Data were processed using the FELIX software package (Molecular Simulations, Inc.).

Determination of thiol groups in 7. Compound **7** (0.34 mg, 0.2 μmol) was dissolved in $CHCl_3$ containing one equivalent of 2,2′-dithiodipyridine (2 mL, 0.1 mM, 0.2 μmol), and the absorbance was monitored at 343 nm to detect formation of 2-thiopyridone.[56, 57] No reaction occurred after 63 h, while upon addition of 2-mercaptoethanol (2 μL), 2-thiopyridone was observed within 0.5 h.

Attempted regeneration of cystine monomer 5-SS by DMSO oxidation of 5-SH: Dithiol **5-SH** (5 mg, 5.9 μmol) was dissolved in 5:4:1 v/v/v H_2O:MeOH:DMSO (5 mL) and left overnight at room temperature.[55] No formation of **5-SS** was detected by either RP-HPLC (C4 column; CH_3CN/H_2O/0.1 % TFA) or ESI-MS.

Acknowledgments

We thank Amir Hoveyda and Michael S. Visser for providing the sample of Ru^{II} catalyst **II** used in these studies, and Mallika Sastry, Julius Rebek, Jr., Robert H. Grubbs, Scott J. Miller, and Hellen E. Blackwell for helpful discussions. This work was supported by the Office of Naval Research (N00014-94-1-0365) and the National Institutes of Health (GM 52190). K.K. acknowledges the Ministry of Education, Science, and Culture of Japan for postdoctoral fellowship support. T.D.C. is the recipient of an NSF predoctoral fellowship.

[1] D. Philp, J. F. Stoddart, *Angew. Chem.* **1996**, *108*, 1242 – 1286; *Angew. Chem. Int. Ed. Engl.* **1996**, *35*, 1154 – 1196.
[2] J. S. Lindsey, *New. J. Chem.* **1991**, *15*, 153 – 180.
[3] *Comprehensive Supramolecular Chemistry*, *Vol. 6: Solid-state Supramolecular Chemistry: Crystal Engineering* (Eds.: D. D. MacNicol, F. Toda, R. Bishop), Elsevier, Oxford, UK, **1996**.
[4] "A chemical template organizes an assembly of atoms, with respect to one or more geometric loci, in order to achieve a particular linking of atoms." D. H. Busch, *J. Incl. Phenom.* **1992**, *12*, 389 – 395.
[5] D. H. Busch, A. L. Vance, A. G. Kolchiksii in *Comprehensive Supramolecular Chemistry. Vol. 9: Templating*, *Self-assembly*, *and Self-organization* (Eds.: J.-P. Sauvage M. W. Hosseini), Elsevier, Oxford, UK, **1996,** pp. 1 – 42.
[6] S. Anderson, H. L. Anderson, J. K. M. Sanders, *Acc. Chem. Res.* **1993**, *26*, 469 – 475.
[7] T. Kogama, *Microbiol. Mol. Biol. Rev.* **1998**, *61*, 212 – 238.
[8] T. Kodadek, *Trends Biochem. Sci.* **1998**, *23*, 79 – 83.
[9] R. B. Freedman, *Curr. Opin. Struct. Biol.* **1995**, *5*, 85 – 91.
[10] T. Zhang, R. Alber, *Nat. Struct. Biol.* **1994**, *1*, 434 – 438.
[11] P. M. Harrison, M. J. E. Sternberg, *J. Mol. Biol.* **1994**, *244*, 448 – 463.
[12] S. F. Betz, *Protein. Sci.* **1993**, *2*, 155 – 158.
[13] S. A. Nepogodiev, J. F. Stoddart, *Chem. Rev.* **1998**, *98*, 1959 – 1976.
[14] N. C. Seeman, *Acc. Chem. Res.* **1997**, *30*, 357 – 363.
[15] D. B. Amabilino, F. M. Raymo, J. F. Stoddart in *Comprehensive Supramolecular Chemistry. Vol. 9: Templating*, *Self-assembly*, *and Self-organization* (Eds.: J.-P. Sauvage, M. W. Hosseini), Elsevier: Oxford, UK, 1996; pp. 85 – 130.
[16] J. D. Hartgerink, T. D. Clark, M. R. Ghadiri, *Chem. Eur. J.* **1998**, *4*, 1367 – 1372.
[17] J. D. Hartgerink, J. R. Granja, R. A. Milligan, M. R. Ghadiri, *J. Am. Chem. Soc.* **1996**, *118*, 43 – 50.
[18] N. Khazanovich, J. R. Granja, D. E. McRee, R. A. Milligan, M. R. Ghadiri, *J. Am. Chem. Soc.* **1994**, *116*, 6011 – 6012.
[19] M. R. Ghadiri, J. R. Granja, R. A. Milligan, D. E. McRee, N. Khazanovich, *Nature* **1993**, *366*, 324 – 327.
[20] H. S. Kim, J. D. Hartgerink, M. R. Ghadiri, *J. Am. Chem. Soc.* **1998**, *120*, 4417 – 4424.
[21] J. R. Granja, M. R. Ghadiri, *J. Am. Chem. Soc.* **1994**, *116*, 10785 – 10786.
[22] M. R. Ghadiri, J. R. Granja, L. K. Buehler, *Nature* **1994**, *369*, 301 – 304.
[23] T. D. Clark, J. M. Buriak, K. Kobayashi, M. P. Isler, D. R. McRee, M. R. Ghadiri, *J. Am. Chem Soc.* **1998**, *120*, 8949 – 8962.
[24] T. D. Clark, M. R. Ghadiri, *J. Am. Chem. Soc.* **1995**, *117*, 12364 – 12365.
[25] K. Kobayashi, J. R. Granja, M. R. Ghadiri, *Angew. Chem.* **1995**, *107*, 79 – 81; *Angew. Chem. Int. Ed. Engl.* **1995**, *34*, 95 – 98.
[26] M. R. Ghadiri, K. Kobayashi, J. R. Granja, R. K. Chadha, D. R. McRee, *Angew. Chem.* **1995**, *107*, 77 – 79; *Angew. Chem. Int. Ed. Engl.* **1995**, *34*, 93 – 95.
[27] M. Saviano, A. Lombardi, C. Pedone, B. Diblasio, X. C. Sun, G. P. Lorenzi, *J. Incl. Phenom.* **1994**, *18*, 27 – 36.
[28] X. C. Sun, G. P. Lorenzi, *Helv. Chim. Acta* **1994**, *77*, 1520 – 1526.
[29] R. H. Grubbs, S. Chang, *Tetrahedron* **1998**, *54*, 4413 – 4450.
[30] R. H. Grubbs, S. J. Miller, G. C. Fu, *Acc. Chem. Res.* **1995**, *28*, 446 – 452.
[31] S. T. Nguyen, R. H. Grubbs, J. P. Ziller, *J. Am. Chem. Soc.* **1993**, *115*, 9858 – 9859.
[32] M. J. Marsella, H. D. Maynard, R. H. Grubbs, *Angew. Chem.* **1997**, *109*, 1147 – 1150; *Angew. Chem. Int. Ed. Engl.* **1997**, *36*, 1101 – 1103.
[33] S. J. Miller, R. H. Grubbs, *J. Am. Chem. Soc.* **1995**, *117*, 5855 – 5856.
[34] S. J. Miller, S.-H. Kim, Z.-R. Chen, R. H. Grubbs, *J. Am. Chem. Soc.* **1995**, *117*, 2108 – 2109.
[35] S.-H. Kim, N. Bowden, R. H. Grubbs, *J. Am. Chem. Soc.* **1994**, *116*, 10801 – 10802.
[36] G. C. Fu, S. T. Nguyen, R. H. Grubbs, *J. Am. Chem. Soc.* **1993**, *115*, 9856 – 9857.
[37] T. E. Creighton, *Biol. Chem.* **1997**, *378*, 731 – 744.
[38] C. B. Anfinsen, *Science* **1973**, *181*, 223 – 230.
[39] L. Moroder, D. Besse, H.-J. Musiol, S. Rudolph-Böhner, F. Sideler, *Biopolymers* **1996**, *40*, 207 – 234.
[40] M. A. Wouters, P. M. G. Curmi, *Proteins: Struct.*, *Funct. Genet.* **1995**, *22*, 119 – 131.
[41] N. Srinivasan, R. Sowdhamini, C. Ramakrishnan, P. Balaram, *Int. J. Peptide Protein Res.* **1990**, *36*, 147 – 155.
[42] P. Raj, S. S. D. Antony, N. Ramasubbu, K. K. Bhandary, M. J. Levine, *Biopolymers* **1990**, *30*, 73 – 85.
[43] H. Balaram, K. Uma, P. Balaram, *Int. J. Peptide Protein Res.* **1990**, *35*, 495 – 500.
[44] I. L. Karle, J. L. Flippen-Anderson, R. Kishore, P. Balaram, *Int. J. Peptide Protein Res.* **1989**, *34*, 37 – 41.
[45] I. L. Karle, R. Kishore, S. Raghothama, P. Balaram, *J. Am. Chem. Soc.* **1988**, *110*, 1958 – 1963..
[46] R. Kishore, P. Balaram, *Biopolymers* **1987**, *26*, 873 – 891.
[47] R. Kishore, A. Kumar, P. Balaram, *J. Am. Chem. Soc.* **1985**, *107*, 8019 – 8023.
[48] R. Kishore, P. Balaram, *J. Chem. Soc.*, *Chem. Commun.* **1984**, 778 – 779.
[49] U. Norikazu, A. Takeo, *J. Am. Chem. Soc.* **1978**, *100*, 4603 – 4605.
[50] C. M. Falcomer, Y. C. Meinwald, I. Choudhary, S. Talluri, P. J. Milburn, J. Clardy, H. A. Scheraga, *J. Am. Chem. Soc.* **1992**, *114*, 4036 – 4042.
[51] A. Ravi, P. Balaram, *Tetrahedron* **1984**, *105*, 2577 – 2583.
[52] A. A. Bothner-By, R. L. Stephens, J. Lee, C. D. Warren, R. W. Jeanloz, *J. Am. Chem. Soc.* **1984**, *106*, 811 – 813.
[53] M. Rance, O. Sørensen, G. Bodenhausen, G. Wagner, R. R. Ernst, K. Wüthrich, *Biochem. Biophys. Res. Commun.* **1983**, *117*, 479 – 485.
[54] B. Kamber, A. Hartmann, K. Eisler, B. Riniker, H. Rink, P. Sieber, W. Rittel, *Helv. Chim. Acta* **1980**, *63*, 899 – 915.
[55] J. P. Tam, C. R. Wu, W. Liu, J. W. Zhang, *J. Am. Chem. Soc.* **1991**, *113*, 6657 – 6661.
[56] T. Stuchbury, M. Shipton, R. Norris, J. P. G. Malthouse, K. Brocklehurst, *Biochem. J.* **1975**, *151*, 417 – 432.
[57] D. R. Grassetti, J. F. J. Murray, *Arch. Biochem. Biophys.* **1967**, *119*, 41 – 49.
[58] S. J. Miller, H. E. Blackwell, R. H. Grubbs, *J. Am. Chem. Soc.* **1996**, *118*, 9606 – 9614.
[59] B. Mohr, M. Weck, J.-P. Sauvage, R. H. Grubbs, *Angew. Chem.* **1997**, *109*, 1147 – 1150; *Angew. Chem. Int. Ed. Engl.* **1997**, *36*, 1308 – 1310.
[60] C. Dietrich-Buchecker, G. Rapenne, J.-P. Sauvage, *Chem. Commun.* **1997**, 2053 – 2054.
[61] H. E. Blackwell, R. H. Grubbs, *Angew. Chem.* **1999**, in press.
[62] T. D. Clark, M. R. Ghadiri, *unpublished results* .
[63] H. F. Gilbert, *Methods Enzymol.* **1995**, *251*, 8 – 28.

[64] J. M. Buriak, M. R. Ghadiri, unpublished results.
[65] A. Rauk, *J. Am. Chem. Soc.* **1984**, *106*, 6517 – 6524.
[66] J. Linderberg, J. Michl, *J. Am. Chem. Soc.* **1970**, *92*, 2619 – 2625.
[67] D. Jiao, M. Barfield, J. E. Combariza, V. J. Hruby, *J. Am. Chem. Soc.* **1992**, *114*, 3639 – 3643.
[68] D. Y. Jackson, D. S. King, J. Chmielewski, S. Singh, P. G. Schultz, *J. Am. Chem. Soc.* **1991**, *113*, 9391 – 9392.
[69] E. K. O'Shea, R. Rutkowski, W. F. I. Stafford, P. S. Kim, *Science* **1989**, *245*, 636 – 648.
[70] E. K. O'Shea, R. Rutkowski, P. S. Kim, *Science* **1989**, *243*, 538 – 542.
[71] C. R. Allerson, G. L. Verdine, *Chem. Biol.* **1995**, *2*, 667 – 675.
[72] A. E. Ferentz, T. A. Keating, G. L. Verdine, *J. Am. Chem. Soc.* **1993**, *115*, 9006 – 9014.
[73] S. M. Davidson, Y. Liu, S. L. Regen, *J. Am. Chem. Soc.* **1993**, *115*, 10104 – 10110.

Received: September 21, 1998 [F 1357]

0947-6539/99/0502-0792 $ 17.50+.50/0